Electronic Supplementary Information

Trace High-Entropy Doping Unlocks High-Energy, High-Rate and Stable Mn-based NASICON Cathode for Sodium-Ion Batteries

Xiaoteng Zhang, †[a] Hao Fan, †[b] Lei Zhang,[a,b] Wenchao Shi,[b] Ping Hu,[c] Ruohan Yu*[a] and Liang Zhou*[a,b]

[1] The Sanya Science and Education Innovation Park, Wuhan University of Technology, Sanya 572000, P. R. China

[2] State Key Laboratory of Advanced Technology for Materials Synthesis and Processing, Wuhan University of Technology, Wuhan 430070, P. R. China

[3] Hubei Key Laboratory of Micro-Nanoelectronic Materials and Devices, School of Microelectronics, Hubei University, Wuhan 430062, P. R. China

*Corresponding author. E-mail: yuruohan@whut.edu.cn, liangzhou@whut.edu.cn

Experimental Section

Materials synthesis. The HE-$Na_{3.14}$MTP was synthesized by a spray drying method. Firstly, 5 g of anhydrous citric acid, 0.1 mmol of ammonium metavanadate, 0.1 mmol of iron nitrate nonahydrate, 0.1 mmol of aluminum nitrate nonahydrate, 0.1 mmol of chromium nitrate nonahydrate, 0.1 mmol of copper acetate monohydrate, 4.5 mmol of dihydropyridine bis (ammonium lactate) titanium, 5.0 mmol of manganese acetate tetrahydrate, 15.7 mmol of sodium acetate anhydrous, and 15 mmol of ammonium phosphate monobasic were dissolved in deionized water under continuous stirring. The above solution was the spray dried at 110 ^{o}C to obtain a light yellow powder precursor. The resulting precursor was calcined at 650 °C for 12 h in an argon atmosphere at a ramping rate of 5 °C min^{-1} to form the carbon-modified HE-$Na_{3.14}$MTP. For NMTP, the synthetic procedure was the same except that the stoichiometric ratios of the reactants were different.

Structure characterization. X-ray diffraction (XRD) measurements were performed on a Bruker D8 Discover utilizing the X-ray diffractometer with Cu Kα X-ray source (λ = 1.5406 Å). Thermogravimetric analysis (TGA) tests were performed using a STA-449C thermogravimetric analyzer in an air with a ramp rate of 10 °C min^{-1}. Raman spectroscopy was performed with the Horiba LabRAM HREvolution. Scanning electron microscope (SEM) images were collected using a JEOL-7100F microscope. Transmission electron microscopy (TEM) images and energy dispersive spectroscopy (EDS) mappings were collected on a JEOL JEM - 2100F STEM/EDS microscope. X-ray photoelectron spectroscopy (XPS) spectra were collected with a VG Multilab 2000. An ASAP 2020 analyser was used to acquire nitrogen adsorption-desorption isotherms to assess the BET specific surface area and pore size distribution of the materials.

Electrochemical Characterization. The electrochemical properties were tested with CR2016 coin-type cells. The cathode was fabricated by pressing a slurry containing active material (70 wt.%), acetylene black (20 wt.%), and polyvinylidene fluoride (10 wt.%) in N-methyl-2-pyrrolidone onto an aluminum foil and dried under vacuum at 70 °C for 12 h. The areal mass loading of active material was approximately 1.2–2.0 mg cm^{-2}. Sodium disks were employed as the counter and reference electrodes; 1.0 M $NaClO_4$ in ethylene carbon/propylene carbonate (1:1 w/w) with 5% fluoroethylene carbonate (electrolyte additive) was used as the electrolyte; Whatman GF/D glass fibre

diaphragm was used as the separator. Galvanostatic charge/discharge testing in the 1.5-4.3V vs. Na/Na^+ potential window was carried out using a multi-channel battery tester (LAND CT2001A). Cyclic voltammetry (CV) tests and electrochemical impedance (EIS) tests at frequencies ranging from 0.1 Hz to 100 kHz were performed using the Autolab PGSTAT 302N electrochemical workstation. For GITT measurements, data collection was based on a procedure with a charge/discharge current of 0.1 C that lasted for 30 min, then followed by a relaxation time of 2 h to reach the stable states.

In-situ XRD experiments during electrochemical testing were performed on a D8 Discover X-ray diffractometer equipped with a planar detector. The cathode containing active material (70 wt.%), acetylene black (20 wt.%), and polytetrafluoroethylene (10 wt.%) was cut into square slices with an area of 1 cm^2 and a thickness of 0.15 mm. The cathode was placed on the backside of an X-ray transparent Be window which also served as the current collector. The in-situ XRD signals were collected in the 2θ range of 18º to 38º with a still mode during the charge/discharge processes; each pattern was acquired in 120s.

In the fabrication of HC//HE-$Na_{3.14}$MTP full cells, the HC electrodes were composed of 80 wt% hard carbon (KURANODE), 10 wt% Super P, and 10 wt% polyvinylidene fluoride (PVDF), using NMP (N-Methyl-2-pyrrolidone) as the solvent. Considering the cathode loadings, the anode HC loading was controlled to be 1.0–1.5 mg cm^{-2}. Since the HeE-$Na_{3.14}$MTP consumes an additional amount of sodium ions during the initial discharge process, it is necessary to perform the pre-sodiation for the HC anode before assembling the full battery. The HC half-cell was cycled at 20 mA g^{-1} for 10 cycles to stabilize the electrode, and then discharged to 0.1 V for a pre-sodiation before full cell assembly. The electrochemical performance of the HC//HE-$Na_{3.14}$MTP full cell was obtained in the voltage range of 1.5 – 4.3 V.

Calculation of configurational entropy

Defining High Entropy Materials

$$\Delta S_{conf} = -R\left[\left(\sum_{i=1}^{N} x_i \ln x_i\right)_{cation} + \left(\sum_{j=1}^{N} x_j \ln x_j\right)_{cation}\right] \qquad \text{(S1)}$$

Where R denotes the universal gas molar constant (R = 8.314). x_i and x_j are the molar fractions of anions and cations, respectively, and N represents the number of elemental species. Expanding the number of elements in a system leads to an increase in S_{conf}. In a system comprising five cations of equal atomic ratio, the highest achievable S_{conf} value stands at 1.61 R. Following the classification based on configurational entropy, materials with $S_{conf} \geqslant 1\ R$ are categorized as "medium entropy," whereas those with $S_{conf} \geqslant 1.5\ R$ fall under the "high entropy" regime.[1] Consequently, high entropy systems intentionally amalgamate a substantial proportion of various elements in roughly equal quantities, thereby creating materials with significant configurational entropy. In this work, the configurational entropy per mole is:[2]

$$\Delta S_{conf} = -R\left(x_{Cr}lnx_{Cr} + x_{V}lnx_{V} + x_{Fe}lnx_{Fe} + x_{Al}lnx_{Al} + x_{Cu}lnx_{Cu}\right) \quad \text{(S2)}$$

$$= 1.61\text{R}$$

Experimental section supplement.

Calculation of sodium ion diffusion coefficient.

GITT: The apparent diffusion coefficient of Na^+ can be calculated based on formulal:[3]

$$D_{\text{Na}^+} = \frac{4}{\pi\tau}\left(\frac{m_B V_M}{M_B S}\right)\left(\frac{\Delta E_S}{\Delta E_\tau}\right) \quad \text{(S3)}$$

where τ corresponds to the constant current pulse time (s); m_B, V_M and M_B are the mass, molar volume, and molar mass of the active material, respectively; and S is the area of the electrode; ΔE_S is the difference between two consecutive stable voltages after relaxation, and $\Delta E\tau$ is the voltage difference between the start and end during a single titration step.

EIS: The Warburg impedance is associated with the diffusion of Na^+ within the electrode. Consequently, D_{Na^+} can be determined through electrochemical impedance spectroscopy. The calculation formula is as follows:

$$D_{Na^+} = \frac{R^2T^2}{2n^4F^4A^2C^2\sigma^2} \quad \text{(S4)}$$

where R, T, n, F, A and C are gas constant, absolute temperature, number of electron transfer per molecule, Faraday constant, surface area of the electrode, and the concentration of Na^+, respectively. And σ is the Warburg factor, which has a relationship with Z' as follows:

$$Z' \propto \sigma\omega^{-1/2} \quad \text{(S5)}$$

where ω is the angular frequency. Therefore, the low-frequency area of EIS plots can be fitted to obtain the Warburg factor. Therefore, the larger the Warburg factor is, the smaller the sodium ion diffusion rate is.

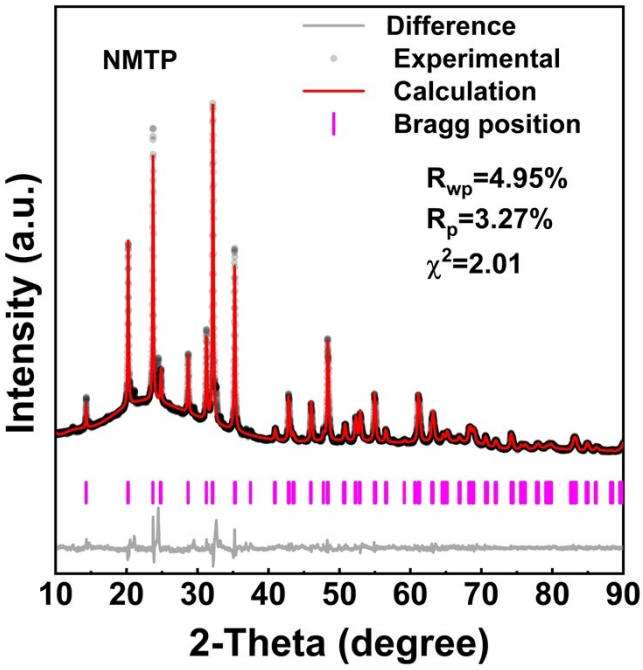

Fig. S1 Rietveld refinement of the XRD pattern of NMTP.

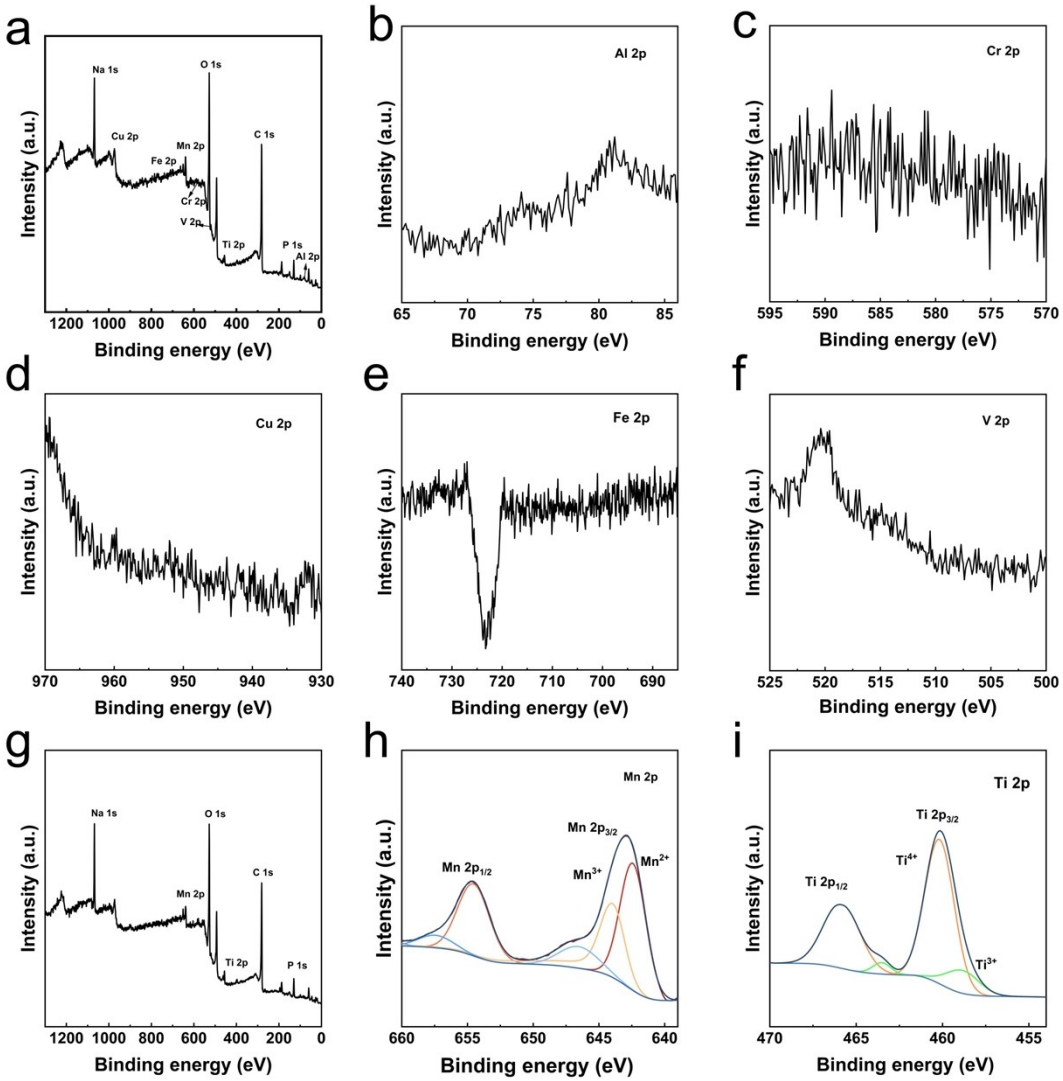

Fig. S2 (a) XPS survey spectrum and high-resolution XPS spectra for the (b) Al, (c) Cr, (d) Cu, (e) Fe and (f) V elements of the HE-$Na_{3.14}$MTP. (g) XPS survey spectrum and high-resolution XPS spectra for the (h) Mn and (i) Ti elements of the NMTP.

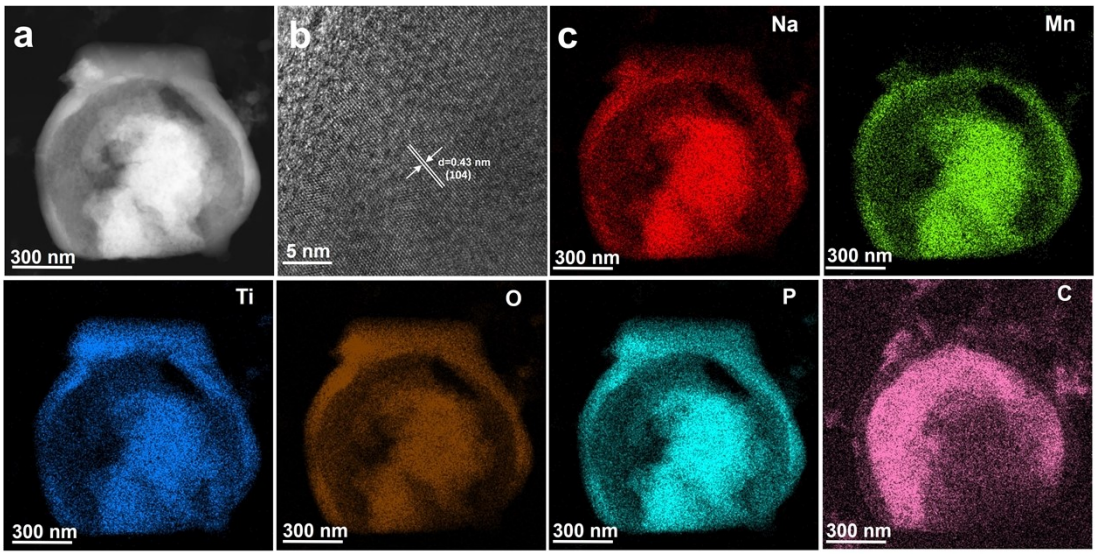

Fig. S3 (a) TEM image, (b) HRTEM image, and (c) the corresponding elemental mappings of Na, Mn, Ti, O, P, and C elements for NMTP.

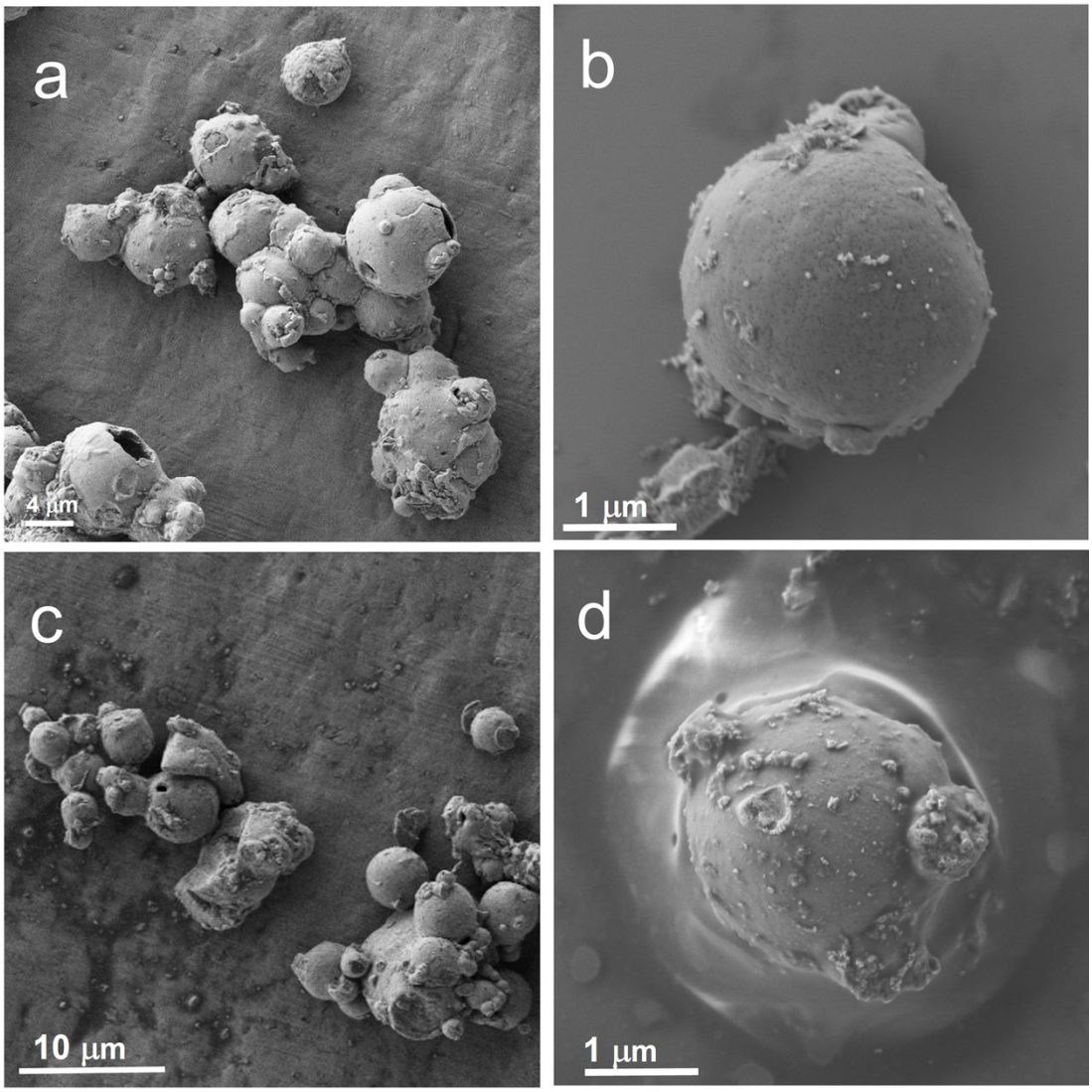

Fig. S4 SEM images of (a, b) HE-$Na_{3.14}$MTP and (c, d) NMTP.

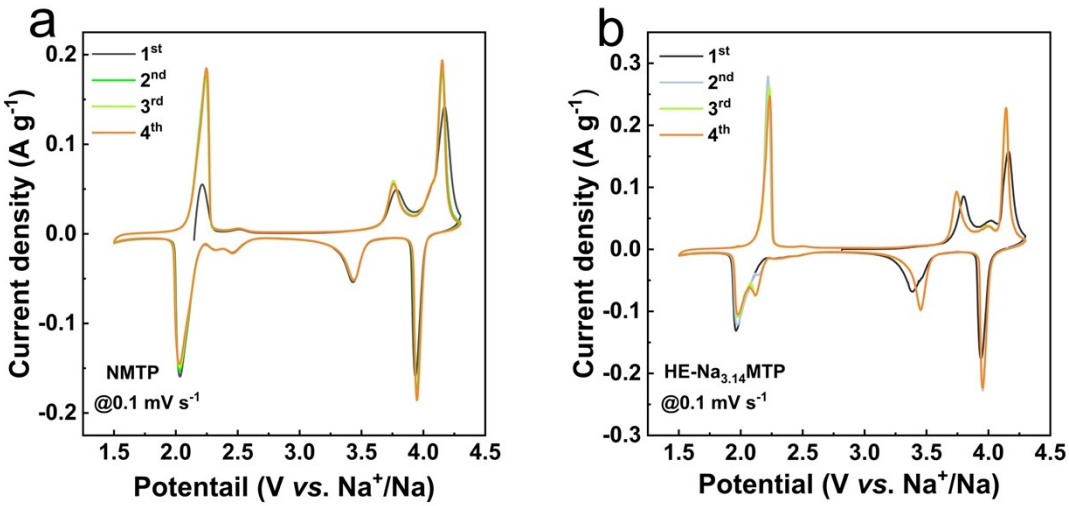

Fig. S5 CV profiles of (a) NMTP and (b) HE-$Na_{3.14}$MTP at 0.1 mV s^{-1}.

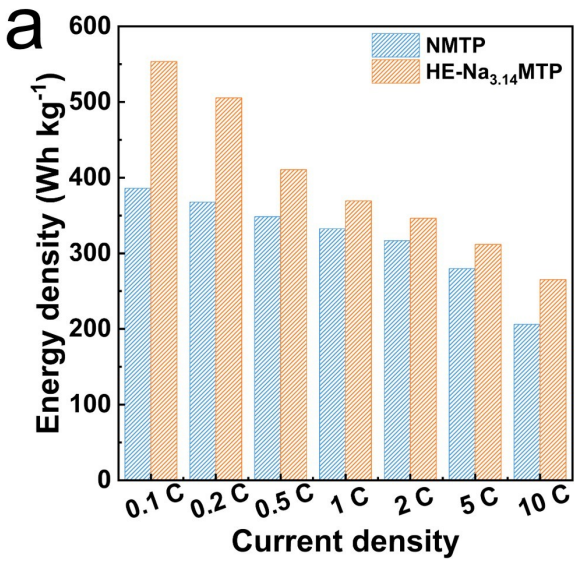

Fig. S6 (a) The energy density of NMTP and HE-$Na_{3.14}$MTP from 0.1 C to 10 C.

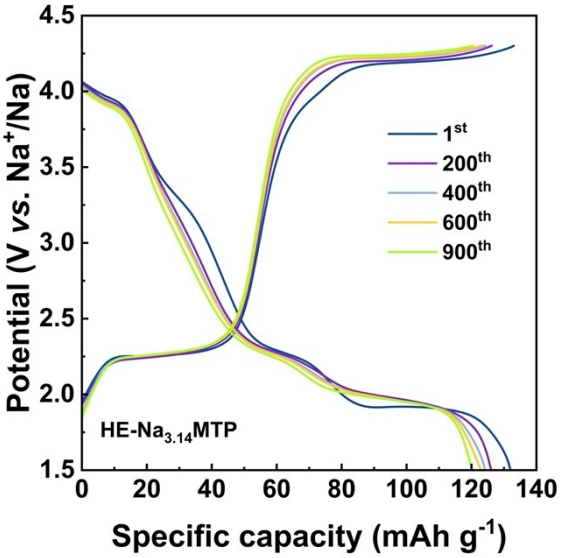

Fig. S7. Galvanostatic charge-discharge (GCD) profiles of HE-$Na_{3.14}$MTP at 5 C rate for cycles 1 to 900.

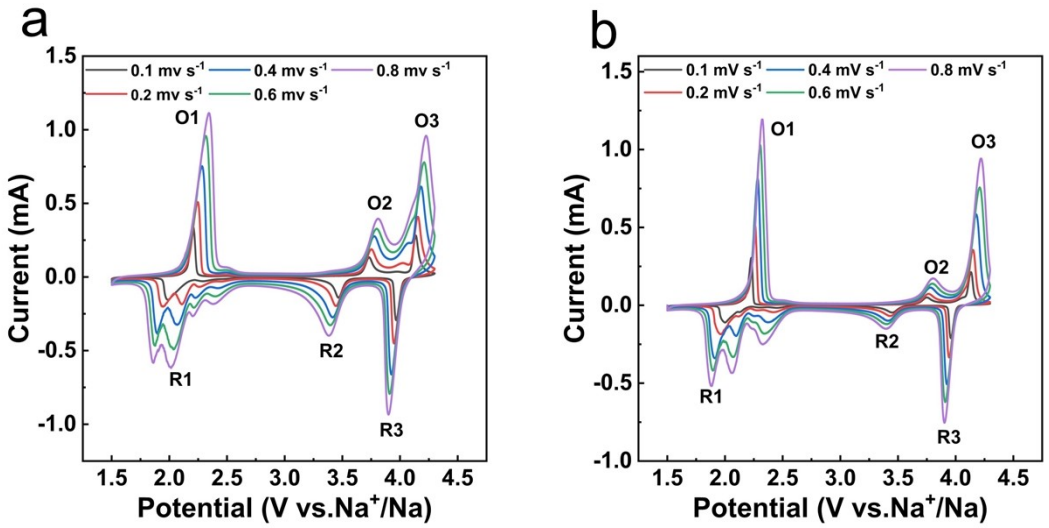

Fig. S8 CV plots of (a) HE-$Na_{3.14}$MTP and (b) NMTP at different scan rates.

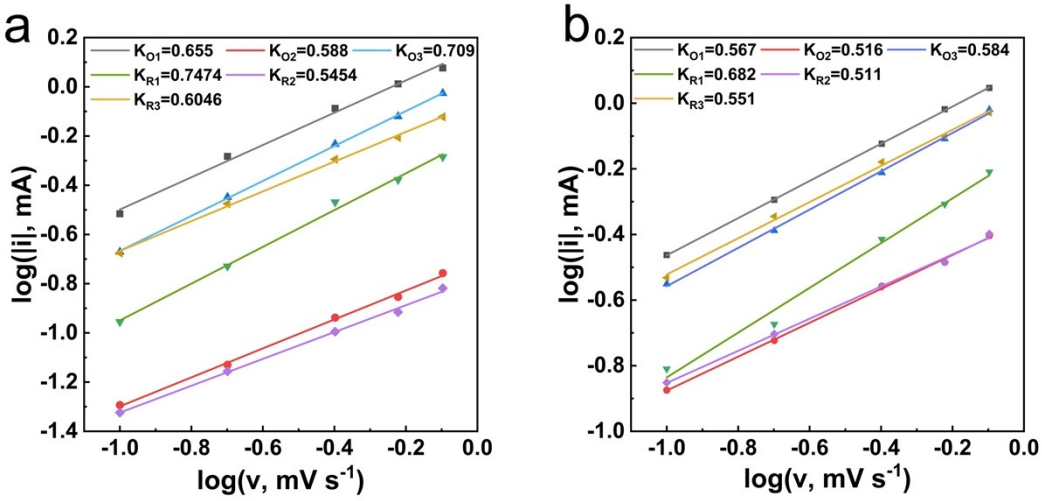

Fig. S9 The log (*i*) versus log (*v*) plots of (a) HE-$Na_{3.14}$MTP and (b) NMTP.

Table S1. Structural parameters of NMTP determined by the Rietveld refinement.

Space group=*R-3c*		**R_p=2.74%**		**R_{wp}=3.83%**
χ^2=2.01		**a=b(Å)=8.86590**	**c(Å)=21.6377**	**V(Å^3)=1472.96**
Atom	**X**	**Y**	**Z**	**Fraction**
Ti	**0.00000**	**0.00000**	**0.14798**	**0.5**
Mn	**0.00000**	**0.00000**	**0.14948**	**0.449**
Na1	**0.00000**	**0.00000**	**0.00000**	**0.829**
Mn/Na1$^+$	**0.00000**	**0.00000**	**0.00000**	**0.009**
Na2	**0.63677**	**0.00000**	**0.25000**	**0.731**
Mn/Na2$^+$	**0.63677**	**0.00000**	**0.25000**	**0.042**
P	**0.29633**	**0.00000**	**0.25000**	**1**
O1	**0.18914**	**-0.01885**	**0.19241**	**1**
O2	**0.18903**	**0.17093**	**0.08632**	**1**

Table S2. Structural parameters of $Na_{3.14}MTP$ determined by the Rietveld refinement.

Space group=*R-3c*		R_p=3.27%		R_{wp}=4.95%
χ^2=2.01		a=b(Å)=8.86611	c(Å)=21.63576	V(Å^3)=1472.88
Atom	X	Y	Z	Fraction
Ti	0.00000	0.00000	0.14798	0.450
Mn	0.00000	0.00000	0.14948	0.498
Na1	0.00000	0.00000	0.00000	0.781
Mn/Na1$^+$	0.00000	0.00000	0.00000	0.001
Na2	0.63677	0.00000	0.25000	0.779
Mn/Na2$^+$	0.63677	0.00000	0.25000	0.001
V	0.00000	0.00000	0.14948	0.010
Fe	0.00000	0.00000	0.14948	0.010
Al	0.00000	0.00000	0.14948	0.010
Cu	0.00000	0.00000	0.14948	0.010
Cr	0.00000	0.00000	0.14948	0.010
P	0.29633	0.00000	0.25000	1
O1	0.18914	-0.01885	0.19241	1
O2	0.18903	0.17093	0.08632	1

Table S3. In Situ Refined Structural Evolution and Volumetric Expansion of NMTP and $Na_{3.14}MTP$ between 1.5 and 4.3 V

Sample		a (Å)	c(Å)	V(Å)	ΔV(%)	R_{wp}(%)	R_p(%)
NMTP	Charge	8.91	21.20	1491.27		8.27	5.23
		8.30	21.75	1327.93	10.35	6.84	4.91
	Discharge	8.91	21.20	1490.40		8.31	5.22
$Na_{3.14}MTP$	Charge	8.80	21.16	1451.78		8.12	5.20
		8.44	21.76	1330.70	9.31	10.01	7.80
	Discharge	8.84	21.18	1467.06		9.37	5.98

References

1. H. Gao, J. Li, F. Zhang, C. Li, J. Xiao, X. Nie, G. Zhang, Y. Xiao, D. Zhang, X. Guo, Y. Wang, Y. M. Kang, G. Wang and H. Liu, *Advanced Energy Materials*, 2024, **14**, 2304529.
2. P. Zhu, Y. Wang, J. Li and Y. Jin, *Energy Storage Materials*, 2024, **71**, 103650.
3. X. Jian, Q. Shen, X. Zhao, J. Jin, Y. Wang, S. Li, X. Qu, L. Jiao and Y. Liu, *Advanced Functional Materials*, 2023, **33**, 2302200.